


Article

Effect of Annealing Temperature on Microstructure and Properties of DH Steel and Optimization of Hole Expansion Property

Yuhuan Yang^{1,2}, Xiaoyue Ma^{1,2}, Hongzhou Lu³ and Zhengzhi Zhao^{1,2,*} 

¹ Collaborative Innovation Center of Steel Technology, University of Science and Technology Beijing, Beijing 100083, China; m202111278@xs.ustb.edu.cn (Y.Y.); m202221344@xs.ustb.edu.cn (X.M.)

² Beijing Engineering Technology Research Center of Special Steel for Traffic and Energy, University of Science and Technology Beijing, Beijing 100083, China

³ CITIC Metal Co., Ltd., Beijing 100004, China; luhz@citic.com

* Correspondence: zhaozhzhi@ustb.edu.cn

Abstract: In this article, DH steel containing Nb and Nb-Cu above 1000 MPa was designed, and its phase transformation law was analyzed through thermal expansion tests. The influence of annealing temperature on the microstructure and properties of DH steel was studied using a continuous annealing simulation testing machine, SEM, and tensile testing machine. The results showed that under a continuous annealing process, the test steel is composed of ferrite, martensite, a small amount of bainite, and residual austenite. The tensile strength decreases with the increase in annealing temperature, Cu element is dissolved in the matrix which produces solid solution strengthening and results in an increase in the strength of Cu-bearing test steel. Finally, 1180 MPa grade DH steel with excellent comprehensive properties was obtained at an annealing temperature of 840 °C and an overaging temperature of 340 °C. The expansion performance of the experimental steel was studied and optimized. Under the step heating annealing process, the experimental steel is composed of tempered martensite, ferrite, and residual austenite, with smaller differences in hardness between different phases, lower average dislocation density, and better expansion performance. Cu-bearing DH steel achieved an excellent match of strength and plasticity of 1289 MPa × 19.8%, with the hole expansion rate of 21.9% and the loss rate of hole expansion rate of 10%.

Keywords: dual-phase steel with high formability; continuous annealing; microstructure; mechanical properties; hole expanding performance



Citation: Yang, Y.; Ma, X.; Lu, H.; Zhao, Z. Effect of Annealing Temperature on Microstructure and Properties of DH Steel and Optimization of Hole Expansion Property. *Metals* **2024**, *14*, 791. <https://doi.org/10.3390/met14070791>

Academic Editor: Tomasz Tański

Received: 28 May 2024

Revised: 23 June 2024

Accepted: 27 June 2024

Published: 7 July 2024



Copyright: © 2024 by the authors. Licensee MDPI, Basel, Switzerland. This article is an open access article distributed under the terms and conditions of the Creative Commons Attribution (CC BY) license (<https://creativecommons.org/licenses/by/4.0/>).

1. Introduction

In the context of “dual carbon”, automotive steel is required to have high strength to ensure safety, as well as excellent plasticity and formability to meet the weight reduction and forming needs of complex components [1,2]. At the same time, the diverse shapes and service environments of automotive components have led to a diversification of processing and forming methods. Common problems such as cracking [3] and failure [4–6] occur during the stamping process, which puts higher requirements on the formability of automotive steel. Some traditional automotive steel urgently needs to be upgraded and replaced.

Conventional duplex (DP) steel consists of ferrite and martensite, with good strong plasticity and low cost, and is widely used in the automotive field, but due to the limitations of its forming properties, enhanced formability duplex (DH) steel gradually entered the market. DH in the DP based on the appropriate adjustments to the composition and process and thus the introduction of residual austenite (RA), which produces a TRIP effect, which in the optimization of plasticity, but also effectively improves the forming ability to solve the problem of cracking failure in the processing and forming of parts. At the same time, it

also effectively improves the forming ability and can solve the problem of cracking and failure during part processing and forming [7,8]. The Cu element can improve the average strength of ferrite, and increase the volume fraction of residual austenite without reducing its stability, thereby optimizing strength plasticity [9,10]. The Nb element can play a role in refining the grain size of DH steel. The Nb element and its second phase can affect the phase transformation law, residual austenite content, and stability of DH steel, resulting in a huge room for improvement in the performance of DH steel.

Studying and optimizing DH steel has great benefits, as its high formability is beneficial in reducing waste generated during processing such as stamping, and lowering part processing costs. When the plasticity level is similar, the tensile strength of DH steel is higher than that of DP steel, which can support the thinning of parts and achieve lightweight. At the same time, a high safety margin is conducive to the integration of multiple parts, thereby reducing the steps of production processes, stamping forming molds, etc., lowering manufacturing costs, and providing more possibilities for future automotive body design. It conforms to the trend of energy conservation, emission reduction, and green and high-quality development, and has broad application prospects as a new type of high-performance automotive steel [11]. However, current research on DH steel is focused on lower strength levels, with less research on DH steel above 1000 MPa, and studies have shown that the expansion performance of DH needs further optimization [12,13].

This article designs and prepares Nb microalloyed DH steel with and without Cu. Based on the study of phase transformation laws, the influence of continuous annealing process parameters on the microstructure and properties of DH steel is studied. The pore expansion performance of the experimental steel under the optimal continuous annealing process parameters is characterized, and the formability of the experimental steel is optimized using a stepped heating process. DH steel with excellent comprehensive properties is obtained, providing a reference basis for the research and industrial production of high-strength Nb microalloyed DH steel.

2. Materials and Methods

2.1. Law of Phase Transformation

The chemical composition of 0Cu-DH steel and 0.15Cu-DH steel is depicted in Table 1. The raw materials are initially melted in a vacuum smelting furnace, and subsequently cast to form steel ingots. These ingots are heated to 1200 °C for 30 min, then forged to produce elongated forging billets. To facilitate laboratory rolling, the forging billets are cut into rectangular shapes measuring 30 mm in thickness, 80 mm in width, and 100 mm in length.

Table 1. Chemical composition of 0Cu-DH steel and 0.15Cu-DH steel (mass fraction%).

Test Steel	C	Si+Al	Mn	Cr	Cu	Nb
0Cu-DH	0.17–0.22	1.05–1.55	2.05–2.85	0.15–0.35	0.00	0.01–0.05
0.15Cu-DH	0.17–0.22	1.05–1.55	2.05–2.85	0.15–0.35	0.15	0.01–0.05

Thermal expansion instruments were utilized to simulate the temperature–time curves depicted in Figure 1a for two types of steel specimens. Tangents were drawn to the heating segment of the resulting temperature–thermal expansion curve, with the inter-critical points identifying the critical phase transformation points for each test steel. In accordance with industry standard YB/T 5128-2018, a simulation test was conducted on 0.15Cu-DH steel using a thermal dilatometer as depicted in Figure 1b, to determine the CCT curve for 0.15Cu-DH steel. Initially, each test steel was raised to 1100 °C at a rate of 10 °C/s and held for 10 min to fully austenitize the specimens. They were then cooled to room temperature at rates ranging from 0.1 to 80 °C/s, respectively, to yield the expansion–temperature curves for each specimen at each cooling rate. Each cylindrical specimen was cut in half from one-half height along the circular surface and inlaid, and the microstructure of the

cut surface was characterized under SEM to determine its continuous cooling transition curve. At each cooling rate, six positions were randomly selected and measured using a micro-Vickers hardness tester, with results averaged after discarding the maximum and minimum values.

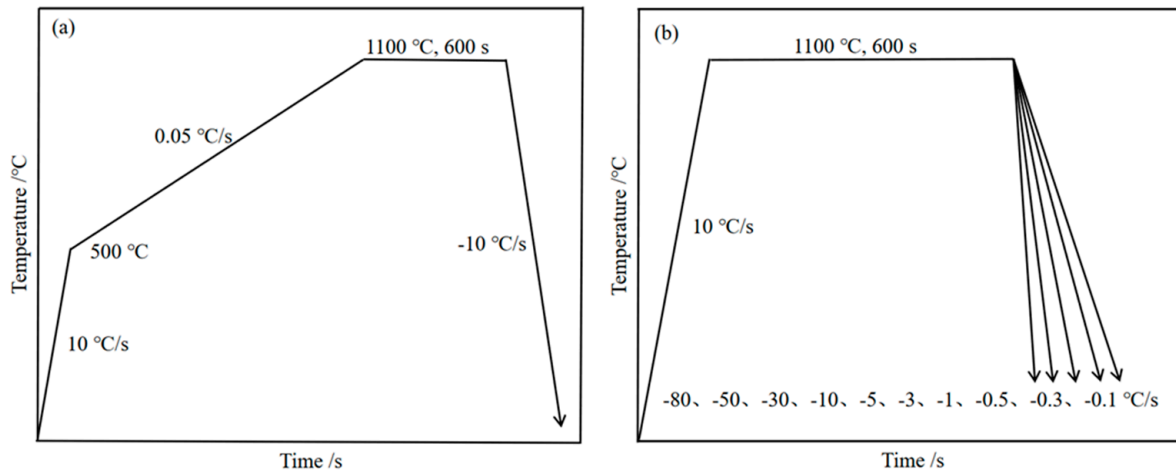


Figure 1. Schematic diagram of the process route for thermal expansion test. (a) Critical point; and (b) CCT curve.

Figure 2a,b depict the expansion–temperature curves determined by DIL 805 thermal dilatometer for the critical points of 0Cu-DH and 0.15Cu-DH steel, respectively. The A_{c1} temperature for 0Cu-DH steel during heating is 686.6 °C, and its A_{c3} temperature is 903 °C, as determined by the tangent method; The A_{c1} temperature for 0.15Cu-DH steel is 647.1 °C, with an A_{c3} temperature of 913.5 °C. The ferrite+austenite two-phase region for 0.15Cu-DH steel is slightly larger than that of 0Cu-DH steel.

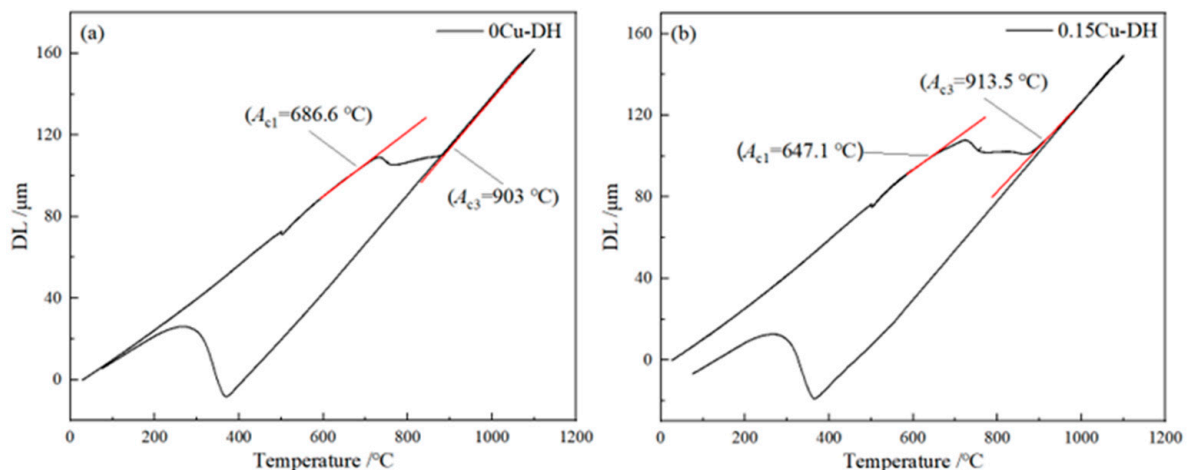


Figure 2. The expansion–temperature curves obtained from measuring the critical points with a thermal dilatometer. (a) 0Cu-DH steel; and (b) 0.15Cu-DH steel.

The CCT curve of the thermal expansion specimen of 0.15Cu-DH steel is depicted in Figure 3. When the cooling rate ranges from 0.1 to 80 °C/s, the steel’s hardness decreases as the cooling rate decreases, correlating with a reduction in martensite and an increase in bainite [14]. At cooling rates between 0.1 and 0.5 °C/s, the steel’s microstructure is predominantly bainite, resulting in a lower hardness of approximately 320 HV1. As the cooling rate increases from 0.5 to 3 °C/s, the martensite content increases, the bainite transformation decreases, and the hardness elevates. When the cooling rate exceeds 5 °C/s,

the steel's microstructure becomes entirely martensitic [15], exhibiting a high hardness exceeding 460 HV1. B is the bainite transformation phase region and M is the martensite transformation phase region.

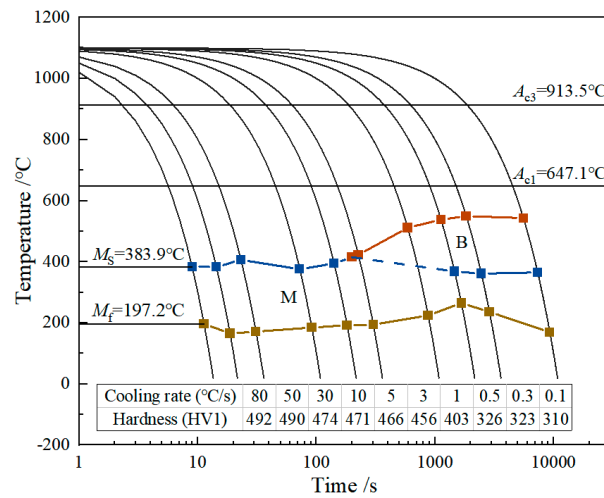


Figure 3. CCT curve of 0.15Cu-DH steel.

2.2. Preparation of Test Steel and Research Methods

Based on the phase transformation laws of experimental steel, a hot rolling process route is designed as depicted in Figure 4. Each experimental steel was subjected to simulated coiling at 700 °C to achieve varying hot rolling microstructure and precipitation behaviors. The hot rolling process involves first uniformly heating the forged billet at 1250 °C for an hour in a muffle furnace, then cooling it to the rolling temperature of 1150 °C. Subsequently, following 5 passes of hot rolling, the forged billet is reduced to approximately 4.3 mm, with the final rolling temperature at 920 °C. Immediately following the final rolling, the plates are water-cooled to 700 °C and then quickly transferred to a muffle furnace for a constant temperature of 1 h before being removed from the furnace and allowed to cool to room temperature. This process ultimately yields the hot-rolled plates of each test steel, designated as 0Cu-DH and 0.15Cu-DH. Each hot-rolled plate is then pickled with hydrochloric acid until its unoxidized structure becomes visible, followed by several cold rolling passes using a cold rolling mill. The cold rolling reduction rate is maintained at approximately 60%, reducing the thickness to between 1.6 and 1.8 mm. This results in cold rolled plate samples suitable for examining the impact of heat treatment process parameters and strategies.

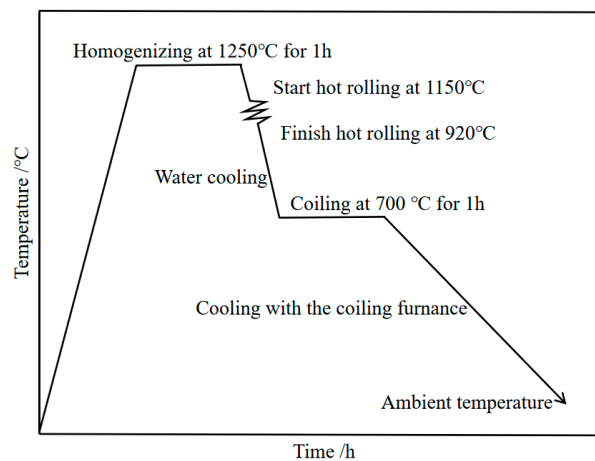


Figure 4. Hot rolling process route.

To achieve a well-matched strength and plasticity in the test steel, the annealing temperature was set within the higher temperature range of the two-phase region, specifically 800–860 °C. To produce the desired amount of bainite and residual austenite, the over-aging temperature was set at 340 °C. The specific process parameters and the process flow chart are depicted in Figure 5a. Specimens were tested for mechanical properties at room temperature using the MTSE45.305 tensile testing machine, with the tensile direction aligned parallel to the rolling direction of the specimens, and the specimens were standardized to A25 dimensions. The microstructure of continuously annealed specimens was analyzed using the Gemini SEM 500 field emission scanning electron microscope (SEM), while the microstructure of DH steel under the stepwise heating annealing process was characterized using the ZEISS ULTRA 55 field emission scanning electron microscope (SEM). The sequence of preparation of each specimen was wire cutting, metallographic inlay, sandpaper grinding, mechanical polishing, cleaning, erosion (4% solution of nitric acid in alcohol), and cleaning and air drying. The highest grit size of metallographic grinding sandpaper used for mechanical polishing was 2000, followed by 2.5 micron polishing paste.

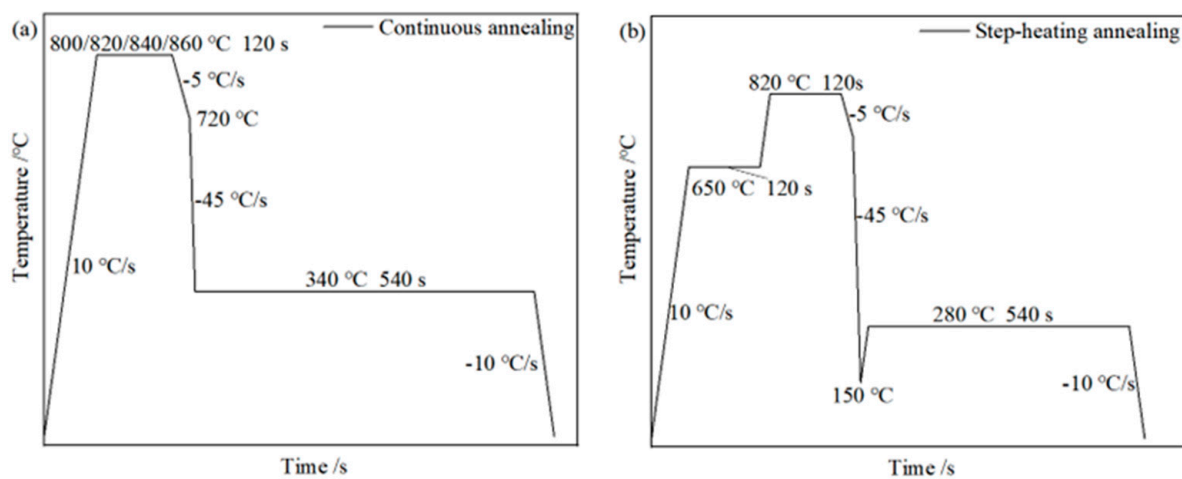


Figure 5. Processing map of heat treatment. (a) Continuous annealing; and (b) step-heating annealing.

Utilizing the BUP600 sheet metal forming testing machine, the hole expansion performance of each test steel was tested under the optimal continuous annealing process parameters. The sample dimensions were $h \times 70 \text{ mm} \times 70 \text{ mm}$, and the hole was punched with a diameter of 10 mm. For reaming, a round hole is punched out using a 10 mm diameter cylinder, after which the hole is enlarged by constant inward squeezing with a conical tool. Under the step-heating annealing process, the test steel is first held below A_{c1} , resulting in a certain degree of recovery and recrystallization, which is beneficial for improving and mitigating the strength and hardness differences between different phases. Therefore, it is expected to optimize the hole expansion performance of the test steel through this process. The specific process parameters are shown in Figure 5b.

3. Results and Discussion

3.1. Microstructure and Properties of 0Cu-DH Steel at Different Annealing Temperatures

The microstructure of 0Cu-DH steel at annealing temperatures between 800 and 860 °C is depicted in Figure 6. The microstructure of the test steel consists of ferrite, martensite, minor amounts of residual austenite, and bainite. At an annealing temperature of 800 °C, due to the lower temperature, some structures in the test steel are not fully recrystallized, with some ferrites appearing in strip form. At annealing temperatures between 820 and 860 °C, the microstructure becomes nearly equiaxed. When the temperature was increased from 820 °C to 840 °C, the proportion of ferrite decreased from 46.4% to 29.4%, the proportion of quenched martensite decreased by 30% [16], and the proportion of tempered martensite and bainite increased, as calculated by Image Pro. Slight tempering of martensite in the

microstructure occurred at an annealing temperature of 800 °C, and the proportion of tempered martensite in the test steel was the largest at 820 °C, reaching 17.1%. At annealing temperatures of 840 °C to 860 °C, the bainite content in the test steel gradually increased from 14.7% to 22.9%. As shown by the XRD statistics, the amount of residual austenite in 0Cu-DH steel at 860 °C reaches 6.2%.

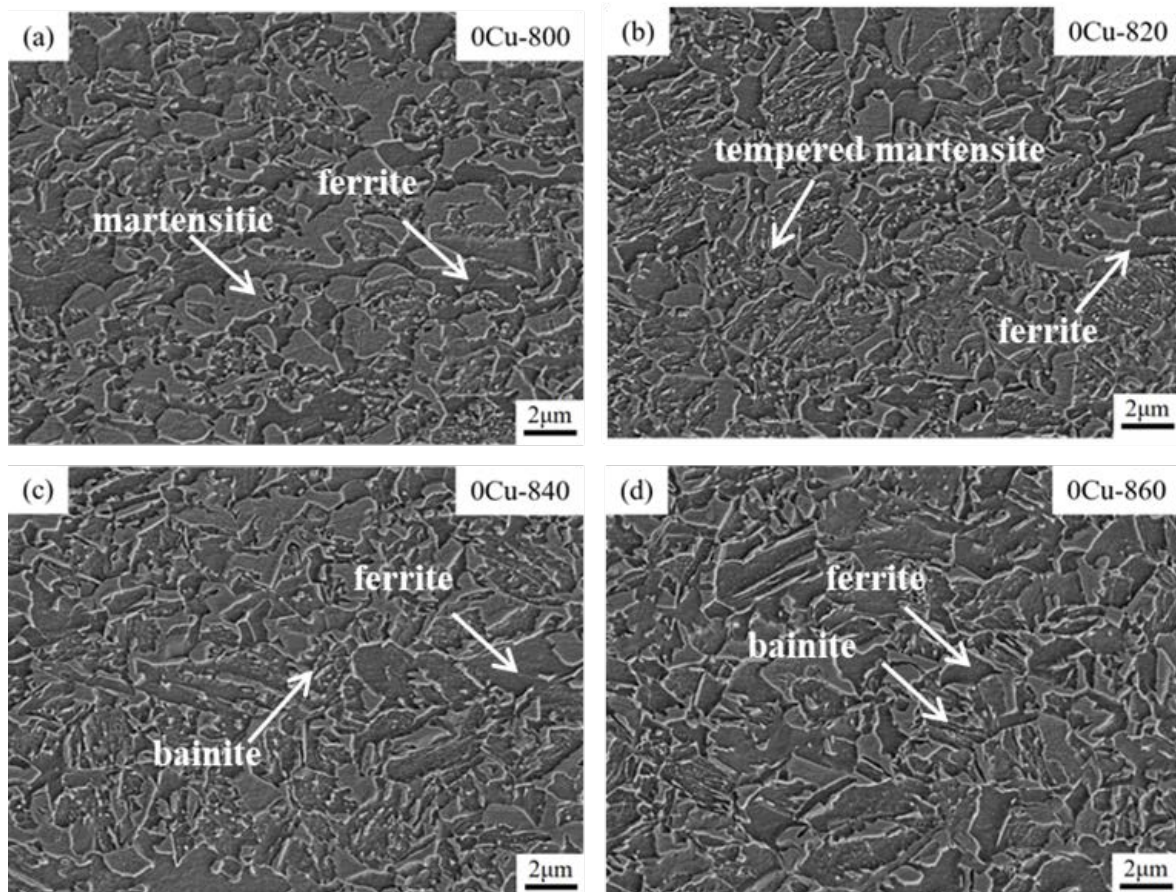
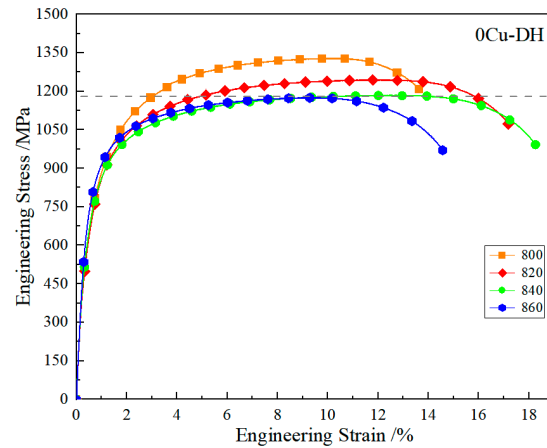


Figure 6. Microstructure of 0Cu-DH steel annealed at 800~860 °C: (a) 800; (b) 820; (c) 840; and (d) 860.

The mechanical properties of 0Cu-DH steel at various annealing temperatures are presented in Table 2 and Figure 7. The dotted line in the figure indicates the 1180 MPa level. As the annealing temperature gradually increases, the yield strength initially decreases and then increases, while the tensile strength decreases from 1328 MPa to 1175 MPa. The elongation initially increases from 13.6% to 18.3% and then decreases to 14.6%. Specifically, when the annealing temperature is raised from 800 °C to 820 °C, there is the greatest decrease in tensile strength and increase in elongation rate for the test steel. However, when the temperature increases from 840 °C to 860 °C, there is minimal change in the tensile strength of the test steel, a significant increase in yield strength, and a marked decrease in elongation rate [17]. In the pre-tempering process, the proportion of hard-phase martensite decreases, while the proportion of tempered martensite increases, which leads to a decrease in yield strength and a decrease in tensile strength; and subsequently continues to increase the heating temperature, the constant increase in bainite and makes the yield strength increase, while the tensile strength continues to decrease. In the 800–840 °C heating process, the reduction of martensite makes the specimen elongation increase, and continuing to raise the heating temperature, the increase in the content of bainite leads to a reduction in its elongation.

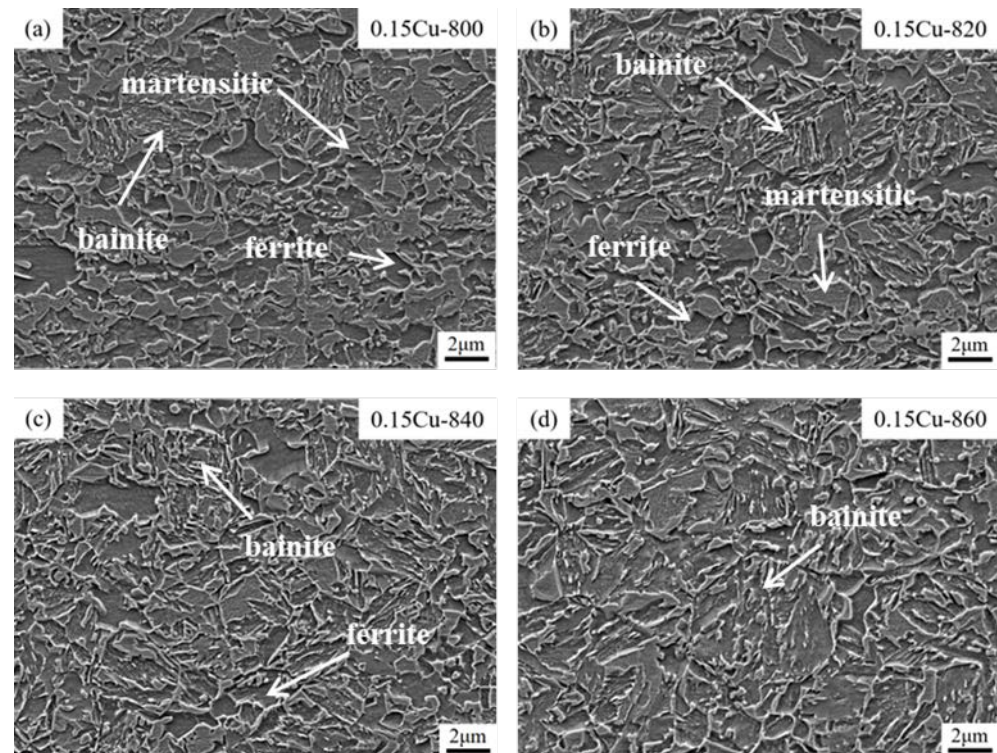
Table 2. Mechanical properties of 0Cu-DH steel annealed at 800~860 °C.

Annealing Temperature/°C	Yield Strength/MPa	Tensile Strength/MPa	Total Elongation/%	Product of Strength and Plasticity/GPa·%
800	672	1328	13.6	18.1
820	628	1245	17.2	21.4
840	655	1184	18.3	21.7
860	749	1175	14.6	17.2

**Figure 7.** Tensile curves of 0Cu-DH steel annealed at 800~860 °C.

3.2. Microstructure and Properties of 0.15Cu-DH Steel at Different Annealing Temperatures

Figure 8 shows the microstructure of 0.15Cu-DH steel during continuous annealing in the annealing temperature range of 800~860 °C.

**Figure 8.** Microstructure of 0.15Cu-DH steel annealed at 800~860 °C: (a) 800; (b) 820; (c) 840; and (d) 860.

At an annealing temperature of 800 °C, some ferrite in the steel assumes strip-like structures. At temperatures between 820 and 860 °C, the microstructure is nearly equiaxed. During the temperature range of 800 to 820 °C, the test steel contains ferrite, quenched martensite, tempered martensite, a minor amount of bainite, and residual austenite. At 840 to 860 °C, further reductions in carbon concentration and alloying elements in the original austenite prevent the formation of quenched or tempered martensite at the elevated overaging temperature of 340 °C, resulting in the test steel being essentially free of martensite and composed of acicular ferrite, bainite, and a small amount of residual austenite. From the XRD analysis, the residual austenite content of 0.15Cu-DH steel increased by 5.9% at 860 °C compared to 800 °C [18]. As the annealing temperature increases, the proportion of bainite in the test steel gradually increases, with bainite being the predominant hard phase at 860 °C. Martensite in 0Cu-DH steel primarily undergoes tempering between annealing temperatures of 820 and 840 °C, while the range for tempering characteristics in 0.15Cu-DH steel is from 800 to 820 °C.

Table 3 and Figure 9 present the mechanical properties of 0.15Cu-DH steel at annealing temperatures ranging from 800 to 860 °C. As the annealing temperature gradually increases, the yield strength initially decreases and then increases, the tensile strength reduces from 1348 MPa to 1265 MPa, and the elongation rate falls from 16.5% to 11.2% [19,20]. At the same annealing temperature, the yield strength and tensile strength of 0.15Cu-DH steel surpass those of 0Cu-DH steel, while the elongation rate does not exhibit a clear trend due to the distinct microstructural transformations between the two grades. Additionally, compared to 0Cu-DH steel, the reduction in tensile strength for 0.15Cu-DH steel is less pronounced as the annealing temperature increases.

Table 3. Mechanical properties of 0.15Cu-DH steel annealed at 800~860 °C.

Annealing Temperature/°C	Yield Strength/MPa	Tensile Strength/MPa	Total Elongation/%	Product of Strength and Plasticity/GPa·%
800	706	1348	16.5	22.2
820	686	1321	15.0	19.8
840	784	1293	11.8	15.3
860	822	1265	11.2	14.2

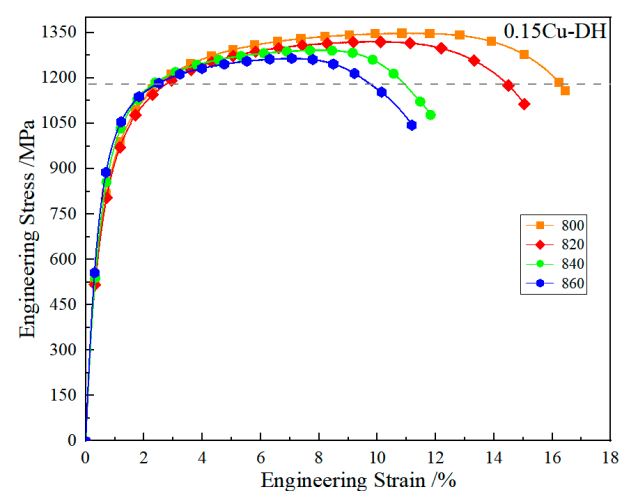


Figure 9. Tensile curves of 0.15Cu-DH steel annealed at 800~860 °C.

3.3. Characterization and Optimization of Hole Expansion Property of Test Steel

Following an exploration of the continuous annealing process parameters and characterization of microstructure and properties, DH1180 test steel with superior mechanical properties was achieved at an annealing temperature of 840 °C and an overaging tem-

perature of 340 °C. Automobile parts are often stamped, placing certain demands on the local formability of the test steel. Consequently, hole expansion tests were conducted on each test steel at an annealing temperature of 840 °C and an overaging temperature of 340 °C to assess its hole expansion capability and to analyze the impact of the time period following punching on this capability [21]. Table 4 presents the hole expansion performance and mechanical properties of the test steel at an annealing temperature of 840 °C and an overaging temperature of 340 °C. The test steel exhibits a favorable expansion rate, ranging from 16.0% to 18.3% [22]. However, extending the time interval between punching and expanding from 0 to 72 h results in a higher rate of loss in the test steel's expansion rate, adversely affecting the actual manufacturing and forming processes.

Table 4. Mechanical properties and hole expansion properties of test steels at annealing temperature of 840 °C and overaging temperature of 340 °C.

Test Steel	Tensile Strength/MPa	Total Elongation/%	Time between Punching and Expanding/h	Hole Expansion Rate/%	Loss of Hole Expansion Rate/%
0Cu-DH	1184	18.3	0	18.3	55.2
			72	8.2	
0.15Cu-DH	1293	11.8	0	16.0	76.2
			72	3.8	

Figure 10 illustrates the microstructure of the experimental steel under the step-heating annealing process, comprising ferrite, tempered martensite, and a minor amount of residual austenite. The overall microstructure retains the banded features of the cold-rolled structure parallel to the rolling direction. The ferrite content in the microstructure of 0Cu-DH steel was calculated by Image Pro to be 13% higher than that of 0.15Cu-DH steel. This is attributed to the steel having been held at 650 °C for 2 min, during which adjacent dislocations merged, opposite dislocations canceled out, and the density of defects dropped significantly [23]. The ferrite in the cold-rolled structure underwent significant recrystallization, and the cementite layers in pearlite became spheroidized. In the subsequent two-phase annealing stage, due to the reduction in nucleation sites and a significant decrease in distortion energy storage in the steel, the distribution of ferrite did not change significantly.

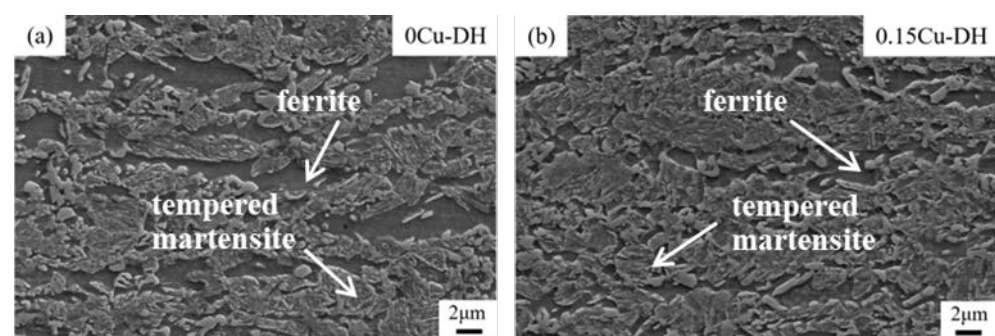


Figure 10. Microstructure of test steels at step-heating annealing process: (a) 0Cu-DH steel; and (b) 0.15Cu-DH steel.

Under the step-heating annealing process, the mechanical properties of the test steel meet the standards of DH1180. The tensile strength of 0Cu-DH steel is 1231 MPa, and the elongation after fracture is 16.0%. The 0.15Cu-DH steel achieves an excellent strength-ductility match of 1289 MPa \times 19.8%, as shown in Table 5 and Figure 11. The hole expansion rates of 0Cu-DH steel and 0.15Cu-DH steel are 19.5% and 21.9%, respectively, which are superior to those of the test steel under the traditional continuous annealing pro-

cess. The rate of hole expansion loss is 21.5% and 10.0%, respectively, which is significantly lower than that under the traditional continuous annealing process.

Table 5. Mechanical properties and hole expansion properties of test steels at step-heating annealing process.

Test Steel	Tensile Strength/MPa	Total Elongation/%	Time between Punching and Expanding/h	Hole Expansion Rate/%	Loss of Hole Expansion Rate/%
0Cu-DH	1231	16.0	0 72	19.5 15.3	21.5
0.15Cu-DH	1289	19.8	0 72	21.9 19.7	10.0

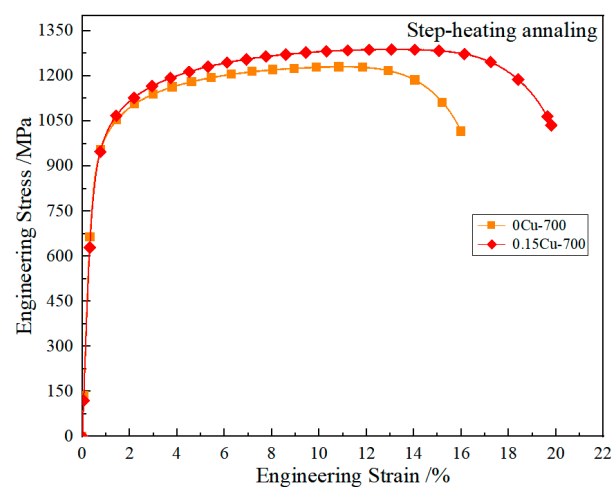


Figure 11. Mechanical properties of test steels at step-heating annealing process.

3.4. Discussion

3.4.1. Effect of Annealing Temperature on Microstructure and Properties of Test Steel

As the annealing temperature gradually increases, the high-strength quenched martensite in 0Cu-DH steel diminishes, leading to a decrease in tensile strength from 1328 MPa to 1175 MPa. At 820 °C, the martensitic tempering characteristics in the test steel become evident. Tempered martensite is favorable for enhancing the elongation at fracture without negatively impacting strength. Consequently, the elongation at fracture shows the largest increase and the largest decrease in tensile strength at this point. At an annealing temperature of 860 °C, the microstructure is predominantly composed of bainite, leading to an increase in yield strength and a decrease in elongation at fracture.

As the annealing temperature increases, the yield strength of 0.15Cu-DH steel initially decreases and then increases, accompanied by a reduction in both tensile strength and elongation at fracture. This correlation can be explained by the relative proportions of each phase in the microstructure of the test steel. As the annealing temperature gradually rises, the primary hard phase transforms from martensite to bainite, leading to a gradual decline in tensile strength. Owing to the higher annealing temperature between 840 and 860 °C, the microstructure is primarily composed of acicular ferrite and bainite, with a more uniform distribution of alloying elements in the original structure [21]. The ferrite contains a higher concentration of alloying elements and is acicular in morphology, resulting in an increase in yield strength and a decrease in elongation at fracture [24,25].

Compared to 0Cu-DH steel, the strength of 0.15Cu-DH steel is higher due to the solid solution strengthening effect of the Cu element. However, at 800 °C, the greater tempering degree of martensite in 0.15Cu-DH steel diminishes its strength advantage; conversely [26], its elongation at fracture exceeds that of 0Cu-DH steel.

3.4.2. Optimization of Step Heating Annealing on Hole Expanding Property of Test Steel

Under the traditional continuous annealing process, each experimental steel exhibits a higher degree of hole expansion [27]. This is attributed to the more uniform distribution of alloy elements in the initial cold-rolled microstructure at higher coiling temperatures, with minimal martensite and a predominance of ferrite and bainite. This results in reduced hardness differences and average hardness among phases, facilitating superior hole expansion performance. However, when the time interval between punching and expanding is extended from 0 to 72 h, the experimental steel experiences a higher rate of loss in hole expansion [28]. This is because punching leaves a significant shear stress gradient around the circular hole, and prolonged exposure leads to hydrogen atom enrichment, resulting in hydrogen embrittlement and compromised hole expansion performance [29].

Under the step-temperature annealing process, the experimental steel's microstructure comprises ferrite, tempered martensite, and minimal residual austenite. The microstructural differences in hardness between phases are markedly reduced compared to those under continuous annealing, leading to a higher degree of hole expansion. Additionally, with a microstructure primarily composed of ferrite and tempered martensite with minimal hardness variations, the stress gradient around the circular hole after punching is reduced [17,30]. Furthermore, the stepwise thermal insulation treatment results in a more uniform distribution of alloying elements and lower average dislocation density within the test steel. This minimizes hydrogen atom enrichment, significantly reducing the rate of hole expansion loss under the step-temperature annealing process and substantially improving hole expansion performance.

4. Conclusions

This article designs Nb microalloyed DH steels with and without Cu, studies their phase transformation laws, and investigates the effects of annealing temperature and Cu element addition on the microstructure and properties of each experimental steel under a continuous annealing process. The expansion performance of the experimental steel is analyzed and optimized, and a 1180 MPa grade DH steel with excellent comprehensive performance is obtained. The following conclusion has been drawn:

(1) We simulated the industrial continuous annealing process route in the laboratory and studied the effect of annealing temperature on the microstructure and mechanical properties of various DH steels. As the annealing temperature gradually increases between 800–860 °C, the content of quenched martensite in each test steel decreases, while the content of tempered martensite or bainite increases. In addition, the average carbon content in the hard phase decreases, resulting in a gradual decrease in the overall strength and hardness of each test steel. A 1180 MPa grade DH steel with excellent comprehensive performance was obtained at an annealing temperature of 820–840 °C. At 840 °C, 0Cu-DH steel achieved the best comprehensive performance of 1184 MPa × 18.3%, with a strength plastic product of 21.7 GPa·%. Cu can be dissolved in the matrix, resulting in solid solution strengthening, and therefore, Cu-bearing DH steel has higher strength.

(2) Under the traditional continuous annealing process, the experimental steel has a good expansion rate, ranging from 16.0% to 18.3%, but the expansion rate significantly decreases with the prolongation of the placement time after punching. Under the step heating annealing process, the microstructure of the test steel is ferrite, tempered martensite, and residual austenite. The hardness difference between the phases is reduced, and the stress gradient around the circular hole after punching is also smaller; Moreover, after stepwise insulation treatment, the distribution of various alloy elements in the microstructure is more uniform, the average dislocation density is lower, and hydrogen atoms are not easily enriched, thus exhibiting excellent pore expansion performance. The 0.15Cu-DH steel achieves an excellent strength plasticity matching of 1289 MPa × 19.8%, while the expansion rate is 21.9% and the loss rate of the expansion rate is only 10%.

Author Contributions: Conceptualization, Y.Y.; Methodology, Y.Y. and X.M.; Software, X.M.; Validation, X.M. and H.L.; Formal analysis, Y.Y. and Z.Z.; Investigation, H.L.; Resources, Y.Y.; Data curation, Y.Y.; Writing—original draft, Y.Y.; Writing—review & editing, Y.Y.; Visualization, Y.Y. and H.L.; Supervision, Z.Z.; Project administration, Z.Z.; Funding acquisition, Z.Z. All authors have read and agreed to the published version of the manuscript.

Funding: This work was supported by the Major Scientific and Technological Innovation Project of CITIC Group (Grant Number 2022zxky06100), and Fundamental Research Funds for the Central Universities (FRF-BD-23-01).

Data Availability Statement: The original contributions presented in the study are included in the article, further inquiries can be directed to the corresponding author.

Conflicts of Interest: Author Hongzhou Lu was employed by the company CITIC Metal Co., Ltd., respectively. The remaining authors declare that the research was conducted in the absence of any commercial or financial relationships that could be construed as a potential conflict of interest.

References

1. Qiao, Y.; Wang, G. Recent Status of Production, Administration Policies, and Low-Carbon Technology Development of China's Steel Industry. *Metals* **2024**, *14*, 480. [[CrossRef](#)]
2. Yao, T.L.; Wu, W.; Yang, Y.; He, Q.; Meng, H.D.; Lin, T.C. Analysis on low-carbon development of China's steel industry under dual-carbon goal. *J. Iron Steel Res.* **2022**, *34*, 505–513. [[CrossRef](#)]
3. Liu, X.L.; Huang, G. Analysis of Factors for the Flange Cracking of Dual Phase Steel. *Eng. Technol. Res.* **2021**, *6*, 13–14. [[CrossRef](#)]
4. Silva, R.C.; Silva, F.; Gouveia, M.R. Investigations on the edge crack defect in Dual Phase steel stamping process. *Procedia Manuf.* **2018**, *17*, 737–17745. [[CrossRef](#)]
5. Yu, L.; Liu, J.; Ge, R.; Wei, X.; Peng, Z.; Chen, M.; Liu, D. Fracture characteristics and mechanism of DP780 duplex steel under different strains. *Forg. Technol.* **2022**, *47*, 48–55.
6. Feng, Y.; Wan, X.M.; Zhou, J.; Xu, W.; Gao, X.; Fang, G.; Yu, C.L.; Zhang, J.P.; Shen, J.; Huang, L.; et al. Research Progress on Fracture Properties of Advanced High-Strength Steel Sheet for Automobiles. *Chin. J. Automot. Eng.* **2023**, *13*, 273–297.
7. Tasan, C.C.; Diehl, M.; Yan, D.; Bechtold, M.; Roters, F.; Schemmann, L.; Zheng, C.; Peranio, N.; Ponge, D.; Koyama, D.; et al. An Overview of Dual-Phase Steels: Advances in Microstructure-Oriented Processing and Micromechanically Guided Design. *Annu. Rev. Mater. Res.* **2015**, *45*, 391–431. [[CrossRef](#)]
8. Zhang, W.; Li, C.G.; Lin, X.M.; Yang, J.W.; Liu, L.X.; Liu, H.S. Analysis of Energy Absorption Characteristics of Dual Phase Steel with High Formability Based on Drop Test. In Proceedings of the 12th CSM steel Congress of the Conference, Beijing, China, 15 October 2019. [[CrossRef](#)]
9. Kim, S.; Lee, G.C.; Lee, T.; Oh, C. Effects of Copper Addition on Mechanical Properties of 0.15C-1.5Mn-1.5Si TRIP-aided Multiphase Cold-rolled Steel Sheets. *ISIJ Int.* **2002**, *42*, 1452–1456. [[CrossRef](#)]
10. Li, H.; Tian, X.; Ren, X. Fatigue fracture behavior and organization analysis of cold-rolled duplex steel. *J. Plast. Eng.* **2023**, *30*, 151–158.
11. Hou, X.; Wang, J.; Ding, M.; Liu, W.; Sun, W.; Kang, H. Influence of matrix organization on the strength-plasticity mechanism of 800 MPa-grade duplex steels. *Met. Heat Treat.* **2022**, *47*, 222–227.
12. Wang, P.; Zhang, Y.; Cai, N.; Fu, C.; Yi, R.; Ju, J.; Chen, W.; Yu, Y. Effect of martensite content on the organization and properties of resistance spot welded joints of alloyed hot-dip galvanized duplex steel. *Precis. Molding Eng.* **2023**, *15*, 160–167.
13. E, H.; Zheng, X.; Li, Y.; Han, L. Prediction of forming limits of DP780 duplex steel based on different instability theories. *Mech. Eng. Mater.* **2022**, *46*, 82–87, 94.
14. Zheng, X.; Tang, D.; Xiao, Y.; Cui, L.; Zhan, H. Influence of annealing process on the reaming properties of 780 MPa Nb-Ti microalloyed duplex steel. *Jiangxi Metall.* **2022**, *42*, 7–11.
15. Lu, H.Z.; Ma, M.T.; Guo, A.M. Development of Automotive EVI Technologies. *Automot. Technol. Mater.* **2022**, 1-9+79. [[CrossRef](#)]
16. Li, H.; Dai, J.; Xian, L.; Liu, X.; Ren, J.; Gao, Y. Effect of annealing temperature on phase transformation and organization of DP590 cold-rolled duplex steel. *Eng. Technol. Res.* **2020**, *5*, 1–4.
17. Wu, X.; Song, Z.; He, J.; Feng, H.; Zheng, W.; Zhu, Y. Effect of N content on the secondary austenite precipitation behavior in S32750 duplex stainless steel. *Spec. Steel* **2024**, *45*, 18–22.
18. Ma, C.; Zhang, D.; Gong, Z.; Liu, X.; Song, H.; Li, D. Study on fracture criterion parameters for toughness of high-strength duplex steel plates. *Mech. Strength* **2023**, *45*, 1474–1482.
19. Cu, S.; Mao, B.; Hu, G. Microstructure modulation and toughening mechanism of advanced high-strength cold-rolled duplex steels for automotive applications. *J. Met.* **2022**, *58*, 551–566.
20. Liu, L.X. Effect of Pre-strain on Microstructure and Mechanical Properties of High Strength Steel DH780. *Hot Work. Technol.* **2022**, *51*, 97–101. [[CrossRef](#)]
21. Luo, R.; Hu, W.; Wang, F.; Tu, J.; Tao, Y.; Shen, W. Effect of aging on the evolution of precipitated phases in super duplex stainless steel. *Spec. Steel* **2024**, *45*, 77–81.

22. Ma, C.; Gao, X.; Xing, L.; Wang, H.; Hu, Z.; Zhai, T. Analysis of stress-strain inhomogeneity during tensile deformation of ferritic/martensitic duplex steels. *Mater. Guide* **2023**, *37*, 178–181.
23. Liu, H.; Yang, S.Y.; Gao, P. Solution to Cracking Problem of 780DH Rear Shock Absorber Support. *Automob. Ind.* **2022**, 36–38.
24. Li, Q.; Ying, C.; Meng, H.; He, L.; Jiang, F. Effects of coiling temperature and cooling rate on microstructure and tensile properties of hot rolled duplex steel containing niobium. *Mech. Eng. Mater.* **2023**, *47*, 45–49+96. [[CrossRef](#)]
25. Cao, L.; Zheng, B.Q.; Wang, Y.C.; Zhou, C.; Yang, Z.M. Influence of acicular ferrite on yielding behavior of HRB400 reinforcing steel bars containing niobium. *China Metall.* **2016**, *26*, 28–32. [[CrossRef](#)]
26. Yang, C.; Xiao, Z.; Feng, Q.; Luo, Z. Study on continuous annealing and organizational properties of high-strength automotive duplex steels. *Precis. Molding Eng.* **2023**, *15*, 168–176.
27. Wang, L.; Fan, L.; Hu, Y.; Zhou, P. Influence of heat treatment process on the organization and properties of S31803 duplex stainless steel. *J. Heat Treat. Mater.* **2023**, *44*, 108–116.
28. Han, L.S.; Ye, S.W.; Zheng, X.B.; Han, Y.; Chen, H.S. Experimental study on hole expansion performance for ultra-high strength dual-phase steel. *Forg. Stamp. Technol.* **2020**, *45*, 187–192. [[CrossRef](#)]
29. Shen, G. Computational Simulation of Organization Evolution during Continuous Annealing of Duplex Steel. Ph.D. Thesis, Shanghai Jiaotong University, Shanghai, China, 2018.
30. Pan, L.; Zuo, Z.; Zhou, W.; Zhu, H. Analysis of forming and fracture limit properties of duplex steels. *Forg. Technol.* **2021**, *46*, 185–189.

Disclaimer/Publisher’s Note: The statements, opinions and data contained in all publications are solely those of the individual author(s) and contributor(s) and not of MDPI and/or the editor(s). MDPI and/or the editor(s) disclaim responsibility for any injury to people or property resulting from any ideas, methods, instructions or products referred to in the content.